Doctoral thesis

Success of a suicidal defense strategy

against infection

in a structured habitat

(なぜ感染で死ぬのか？感染の集団生物学の

「実験＋数理」解析系の創出)

Masaki Fukuyo

Department of Medical Genome Sciences, Graduate School of Frontier Sciences,

University of Tokyo

Table of contents

Table of contents 1

Abstract 3

Introduction 4

Results 8

Experimental design 8

Time course of infection 11

Time course of infection 12

Varying the ratio of the hosts 12

Observation of microcolonies 13

Emergence of host mutants resistant to the pathogen 13

Emergence of pathogen mutants not inducing host death 17

Mathematical modeling and simulation 26

Discussion 34

Materials and methods 36

Bacterial strains, bacteriophage strains, and plasmids 36

Growth medium 41

Bacterial growth 41

Phage preparation and plaque assay 41

Infection 42

Fluorescent microscopy 43

Identification and characterization of mutants 43

Sequence determination 44

Model 44

References 52

Acknowledgments 57

Appendix 58

Supplementary Animations:

Animation S1. Initial A:S = 10^{-3}.

Animation S2. Initial A:S = 10^{3}.

Abstract

Why do some organisms succumb and die easily when infected? Microbial infection often leads to expression of virulence and host death when symbiosis seems more beneficial for the infecting microbe's maintenance. Previously proposed explanations have focused on the pathogen's side. In this work, I tested a hypothesis focused on the host strategy. If a member of a host population dies immediately upon infection with a pathogen, thereby ending its reproduction, then its death could protect the host population from secondary and further infections. I tested this "Suicidal Defense Against Infection" (SDAI) hypothesis by developing an experimental infection system that involves a huge number of bacterial cells as host and their virus as pathogen and is linked to mathematical modeling. I prepared two host strains, one with the SDAI strategy (type A) and the other without (type S), mixed them at varying ratios, challenged them with the pathogen and monitored any change in the ratio during infection. I used two conditions for infection: standing solid agar providing spatial structure, thereby ensuring that individuals preferentially interact with their neighbors, and well-mixed liquid lacking spatial structure. I found that the SDAI strategy has great advantage in the presence of spatial structure: Pathogen increase was accompanied by a large increase in the A:S ratio. In contrast, there was a decrease in the A:S ratio in the absence of spatial structure. My simulation reproduced the essential features of the experimental results. These results provide a new perspective for understanding host-pathogen interaction.

Introduction

Why do some organisms succumb and die easily when infected? Microbial infection often leads to expression of virulence and host death when symbiosis seems more beneficial for the infecting microbe's maintenance. Previously proposed concepts have focused on the pathogen's strategy and they provide only partial explanations, such as better reproduction(1), incomplete adaptation after a host jump(2), and within-host competition(3).

In multicellular organisms, cells infected with pathogens often undergo programmed death to end their propagation and prevent secondary infection of neighboring cells(4). Virulence and transmissibility are negatively correlated in some pathogens, such as influenza virus(5). Based on these considerations, I propose a hypothesis focused on the host strategy. If a member of a host population dies immediately upon infection with a pathogen, thereby ending its reproduction, then its death could protect the host population from secondary and further infections (Fig. 1; Fig. 2*A*). Indeed, bacterial suicide aborting virus (bacteriophage) multiplication has long been known as phage exclusion(6).

I tested this "Suicidal Defense Against Infection" (SDAI) hypothesis by developing an experimental infection system containing a large number (100,000,000) of hosts, which was linked to mathematical modeling and computer simulation. The unicellular bacterium *Escherichia coli* and bacteriophage lambda, well studied for long time, were used as the model host and pathogen. The infection was conducted either in the presence of spatial structure (within soft agar) or its absence (in a well-mixed liquid). My experiments and simulation demonstrated that the SDAI strategy is successful in the presence of spatial structure but unsuccessful in its absence.

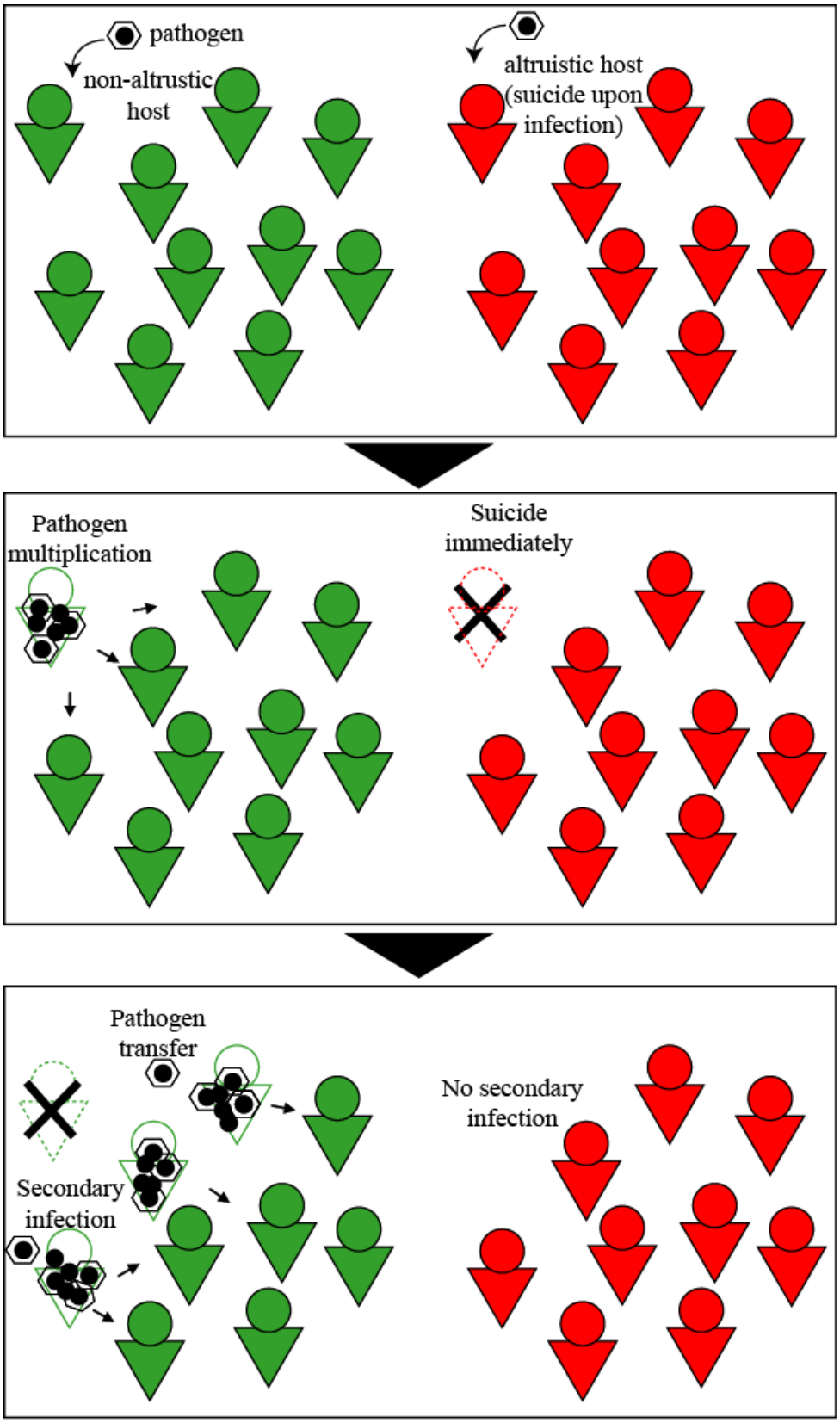
pathogen
non-altrustic host
altruistic host (suicide upon infection)
Pathogen multiplication
Suicide immediately
Pathogen transfer
No secondary infection
Secondary infection

Figure 1. Summary diagram of the success of the Suicidal Defense Against Infection (SDAI) strategy in the presence of spatial structure.

Non-altruistic hosts and altruistic hosts were found in a colony. The non-altruistic colony spreads infection, whereas the altruistic host colony prevents spread of infection due to the altruistic suicide of an infected member.

Results

Experimental design

I prepared two host strains: susceptible type S that allows multiplication of the pathogen when infected (Fig. 2*A*(*i*)) and *altruistic* type A that immediately commits suicide when infected with pathogen P (SDAI strategy, see Introduction) (Fig. 2*A*(*ii*)). The former type without SDAI strategy will be referred to as *non-altruistic* for contrast. The pathogen P (Fig. 2*A*) was bacteriophage lambda carrying a DNA methyltransferase gene(7). Upon entering a host, the methyltransferase produced by this pathogen starts methylating the host genome. A DNase in host A cleaves the genome near the methylated sites, which leads to host death. Host S lacks this DNase. Pathogen Q lacked the DNA methyltransferase and could not induce suicide in either host. These relationships are shown in Fig. 2*B*.

Fig. 2*C* illustrates the experimental procedure. I mixed the two hosts A (altruistic) and S (non-altruistic) at various ratios and infected them with pathogen P, before monitoring any change in the ratio. Spatial structure is important in interaction between organisms (8-14), so I used two infection conditions: standing soft agar provided spatial structure, thereby ensuring that individuals preferentially interacted with their neighbors; a well-mixed liquid where spatial structure was absent, which is expected to allow any individual to interact with any other individual with an equal frequency.

A

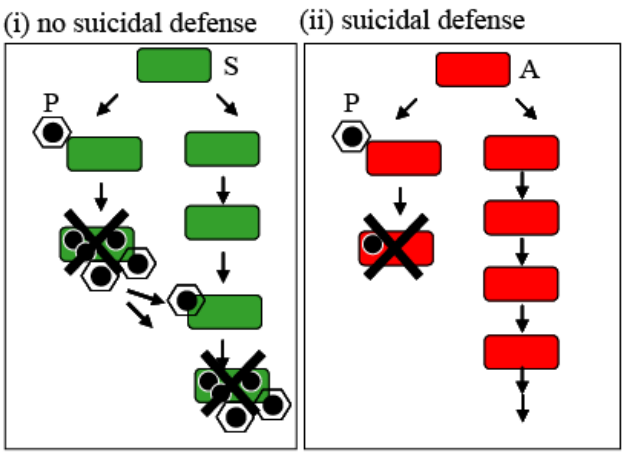

C

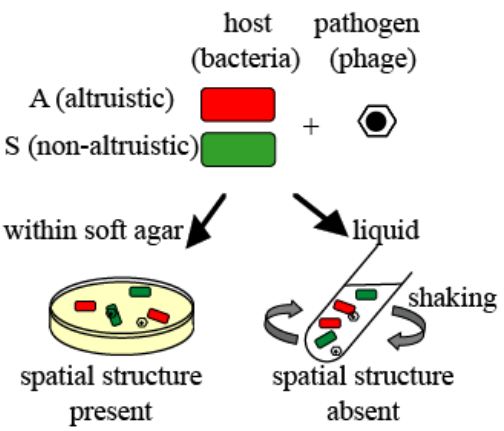

B

Type			Suicide	Number after infection	
Host	Pathogen			Host	Pathogen
S (non-altruistic)	-		-		
S	P	(suicide inducing)	-		
S	Q	(not suicide inducing)	-		
A (altruistic)	-		+		
A	P		+		
A	Q		-		

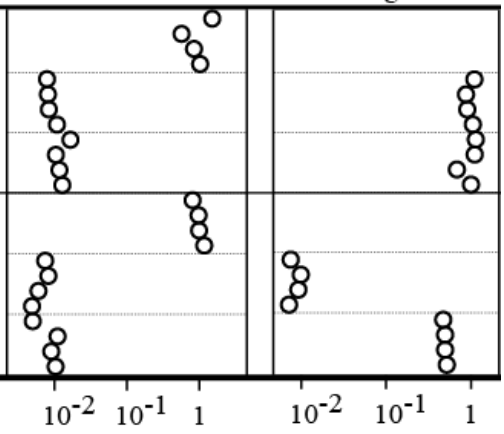

Figure 2. Design. (*A*) Concept of "Suicidal Defense Against Infection" (SDAI). (*i*) A host of the non-altruistic (non-suicidal) type S allows propagation of pathogen P and secondary infection of other hosts. (*ii*) A host of the altruistic (suicidal) type A commits suicide immediately after infection, thereby ending pathogen multiplication and preventing secondary infection of other hosts. (*B*) Survival of the host and the pathogen after infection. The host number (relative colony-forming units) was measured in the presence of excess pathogens. The pathogen number (relative plaque-forming units) was measured in the presence of excess hosts. See Materials and methods for the genotype of the hosts (*Escherichia coli*) and the pathogens (bacteriophage lambda). (*C*) Experimental procedure. The two types of host were mixed at a varying ratio, challenged by the pathogen, and incubated under two different conditions: one with spatial structure and the other without. Change in the ratio was monitored. See Materials and methods for detail.

Time course of infection

The time course of the infection experiments is analyzed in Fig. 3*A*, *B*. In the presence of spatial structure (Fig. 3*A*), pathogen increase was accompanied by a gradual increase in the A:S ratio, eventually by two orders of magnitude (1/1000 to 1/10). This demonstrates that the SDAI strategy facilitated a relative increase in host A. In contrast, pathogen increase was accompanied by a decrease in the A:S ratio when spatial structure was absent (Fig. 3*B*). These results clearly indicated that the infection conditions played an important role in the success of the SDAI strategy. The unexpected decrease in the ratio when spatial structure was absent will be addressed later.

Varying the ratio of the hosts

I then investigated the final A:S ratio as a function of the initial A:S ratio (Fig. 3*E*, *F*) along with a control lacking the pathogen. In the experiments with spatial structure (Fig. 3*E*) and without the pathogen, the ratio changed very little. The slight downward shift of the line without any pathogen is reproducible and might reflect a growth disadvantage of host A. The increase in the A:S ratio in the presence of pathogen P was the largest with the lowest initial A:S ratio (1/1000), and insignificant at the highest A:S ratio (1000). There is negative relationship between relative fitness (rational increase in A:S) of host A (= y) snd the initial A:S ratio (= x). The relationship can be described by a power function $y = 8.3\ x^{-0.28}$, $R^2=0.88$.

In experiments where spatial structure and the pathogen were absent (Fig. 3*F*), the ratio changed very little, although it decreased slightly at the highest initial ratio. With

pathogen P in the absence of spatial structure, the A:S ratio decreased by two orders of magnitude, from 1/1000 to 1/100000. This decrease emphasizes the contrast between the conditions with and without spatial structure.

Observation of microcolonies

Fig. 4*A* and *B* show fluorescent microscope images of the host microcolonies, where the two hosts were labeled using different fluorescent proteins. A and S microcolonies grew normally when the pathogen was not present (Fig. 4*A*). However, S microcolonies were destroyed after infection with pathogen P, whereas A microcolonies grew even when surrounded by the pathogen source (Fig. 4*B*).

Emergence of host mutants resistant to the pathogen

The decrease in A:S ratio in the absence of spatial structure at the low initial ratio might be explained by mutations in the host and/or pathogen, which are expected to occur with this type of experimental infection(15). Thus, I analyzed their genotype after the infection.

In the absence of spatial structure, hosts A and S were found to be replaced by pathogen-resistant mutants after 16 h of incubation. In the presence of pathogen P, the fraction of resistant mutants increased from $2.70 \pm 0.18 \times 10^{-6}$ to 0.94 ± 0.06 for host S and from $3.59 \pm 0.49 \times 10^{-6}$ to $1.11 \pm 0.16 \times 10^{0}$ for host A (n = 4). These results explain the decrease in A:S ratio in the absence of spatial structure at the low initial ratio (Fig. 3*F*, *H*). The host A population was too small to initially harbor the pathogen-resistant

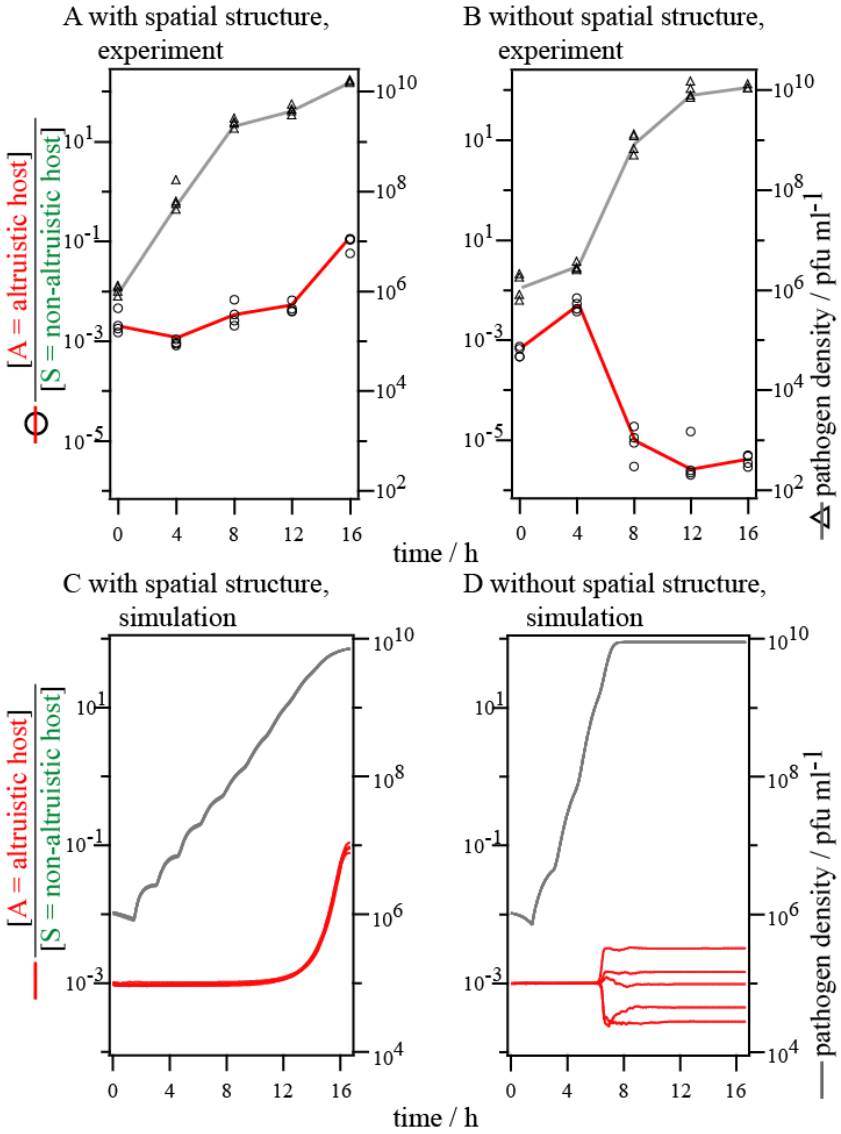
A with spatial structure, experiment
B without spatial structure, experiment
C with spatial structure, simulation
D without spatial structure, simulation
[A = altruistic host] / [S = non-altruistic host]
pathogen density / pfu ml-1
time / h

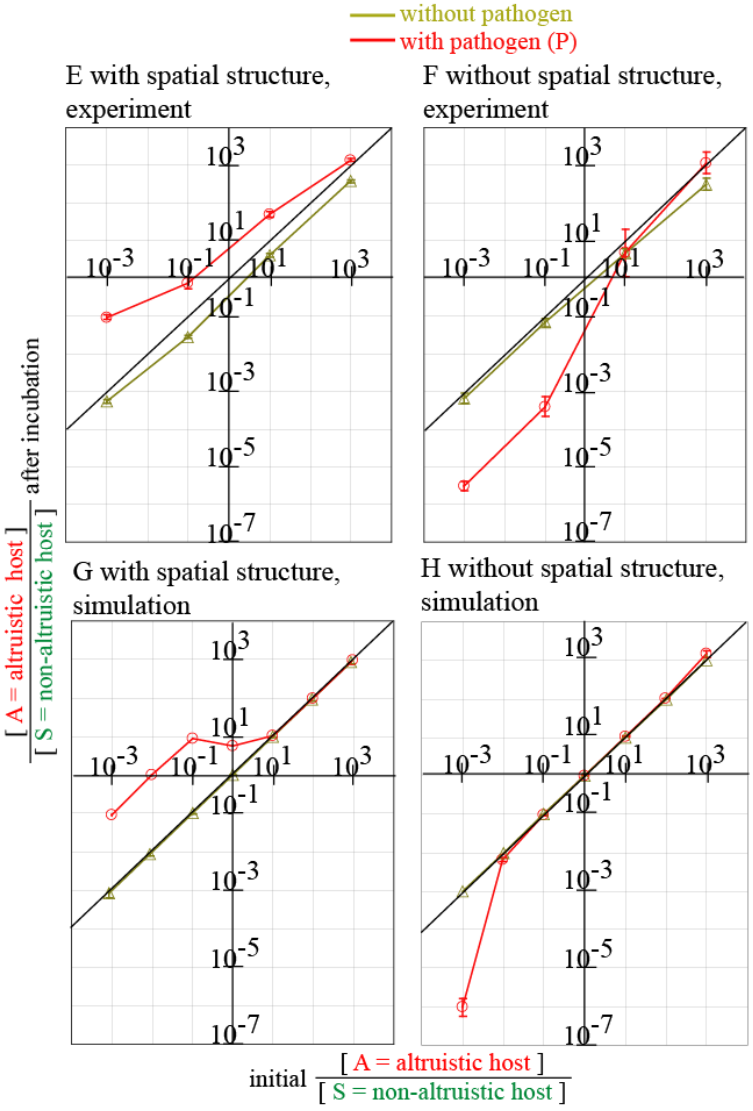
without pathogen
with pathogen (P)
E with spatial structure, experiment
F without spatial structure, experiment
G with spatial structure, simulation
H without spatial structure, simulation
[A = altruistic host] / [S = non-altruistic host] after incubation
initial [A = altruistic host] / [S = non-altruistic host]

Figure 3. Changes in the ratio of the altruistic (suicidal) host to the non-altruistic (non-suicidal) host during infection. (*A-D*) **Time course.** N = 4 in experiments and 5 in simulations. (*E-H*) **Varying input ratio.** The initial ratio of the altruistic (suicidal) host to the non-altruistic (non-suicidal) host was varied (horizontal axis). The ratio was measured after 16 h of incubation in experiments and after a simulation time of 16.7 h (vertical axis). The averages ± SEM (N = 4) are shown for experiments. The results from 100 runs are shown for simulations. (For individual simulation results for *H*, see Figure 7).

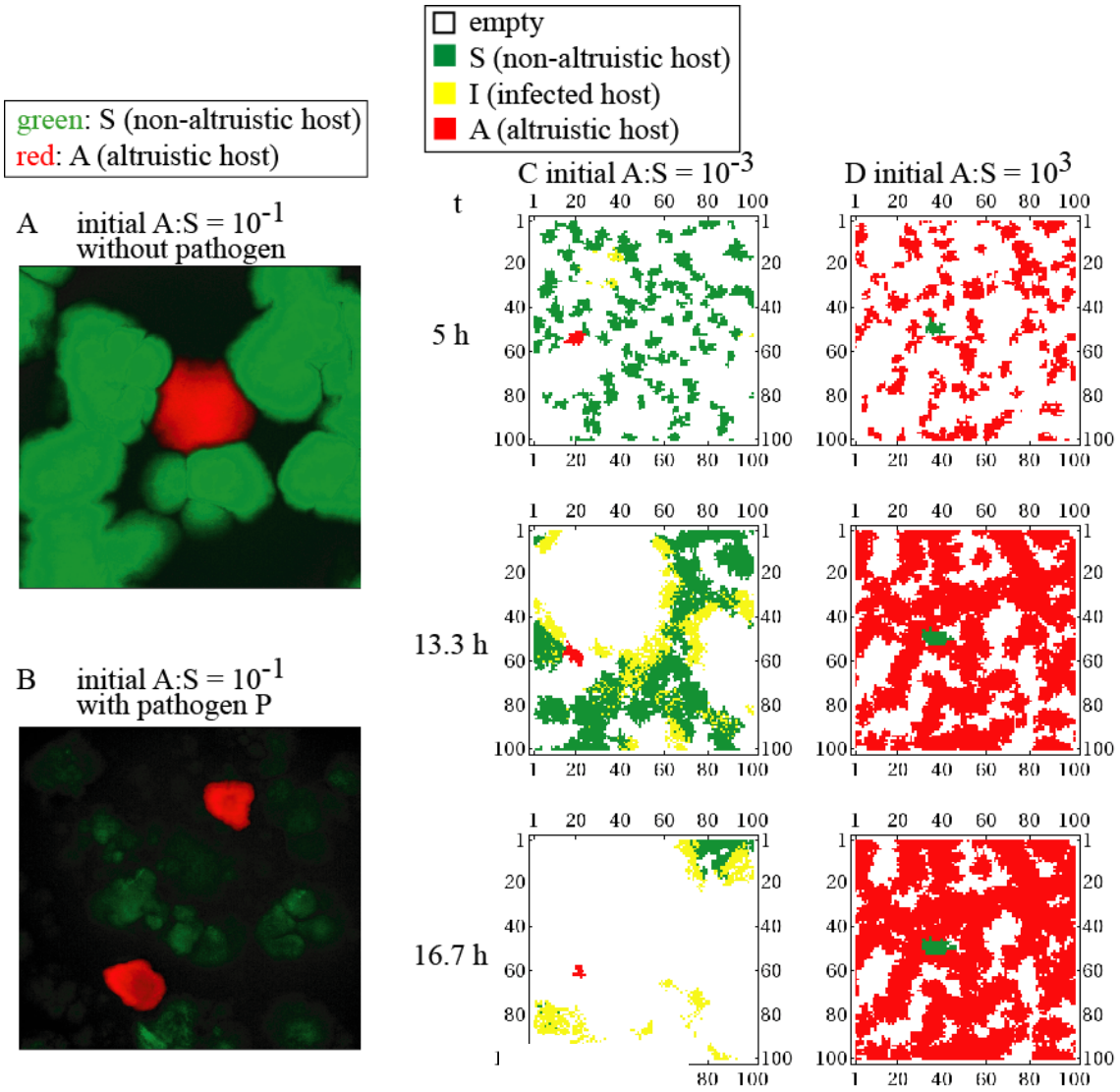

Figure 4. Snapshots in the presence of spatial structure. (*A*), (*B*): from experiments. The non-altruistic host S was labeled with a green fluorescent protein, while the altruistic host A was labeled with a red fluorescent protein (see Materials and methods for detail). 16 h after infection. (*C*), (*D*): from simulation. A 100 × 100 area of the 256 x 256 lattice is shown.

mutants. This point will be confirmed by simulation later.

On the other hand, there is no decrease in S:A ratio(= no increase in A:S ratio) at the low initial S:A ratio (at the high initial A:S ratio) (Fig. 3*F*). Likely because of lack of hosts (S) that allow multiplication of the pathogen, infection does not expand to provide selection for the host mutants. Consistent with this interpretation, host S:A ratio slightly decreased (A:S ratio increased) at the S:A ratio of 1:1000 (A:S ratio of 1000:1) with control pathogen Q, which does not induce host suicide (Fig. 2*B*; Fig. 5)

Emergence of pathogen mutants not inducing host death

After the above infection experiments, I found mutants of pathogen P that were defective in inducing host suicide, just as the control pathogen Q (Fig. 6*A*). These mutants could grow in host A as well as host S (Fig. 6*B,* blue circle). Sequencing showed that they carried different mutations in the methyltransferase gene that induces the suicide (Fig. 6*A*). Each tube used for infection contained multiple mutants (Fig. 6*A*, *B*, Table 1). Methyltransferase activity was estimated based on growth in the presence of restriction enzyme that cleaves the pathogen genome at its unmethylated sites. The activity level varied among the mutants, but it was similar in those mutants from the same tube (Fig. 6*B*, red triangle). Based on these, I estimated the number of mutants defective in inducing host suicide that emerged from the infection process (Fig. 6*C*).

I found that more mutants appeared with a higher initial A:S ratio, which was likely because host A selects them. In the absence of spatial structure and with a high initial

A:S ratio, the pathogen population was entirely replaced by this type of mutants (Fig. 6*C*(*ii*)).

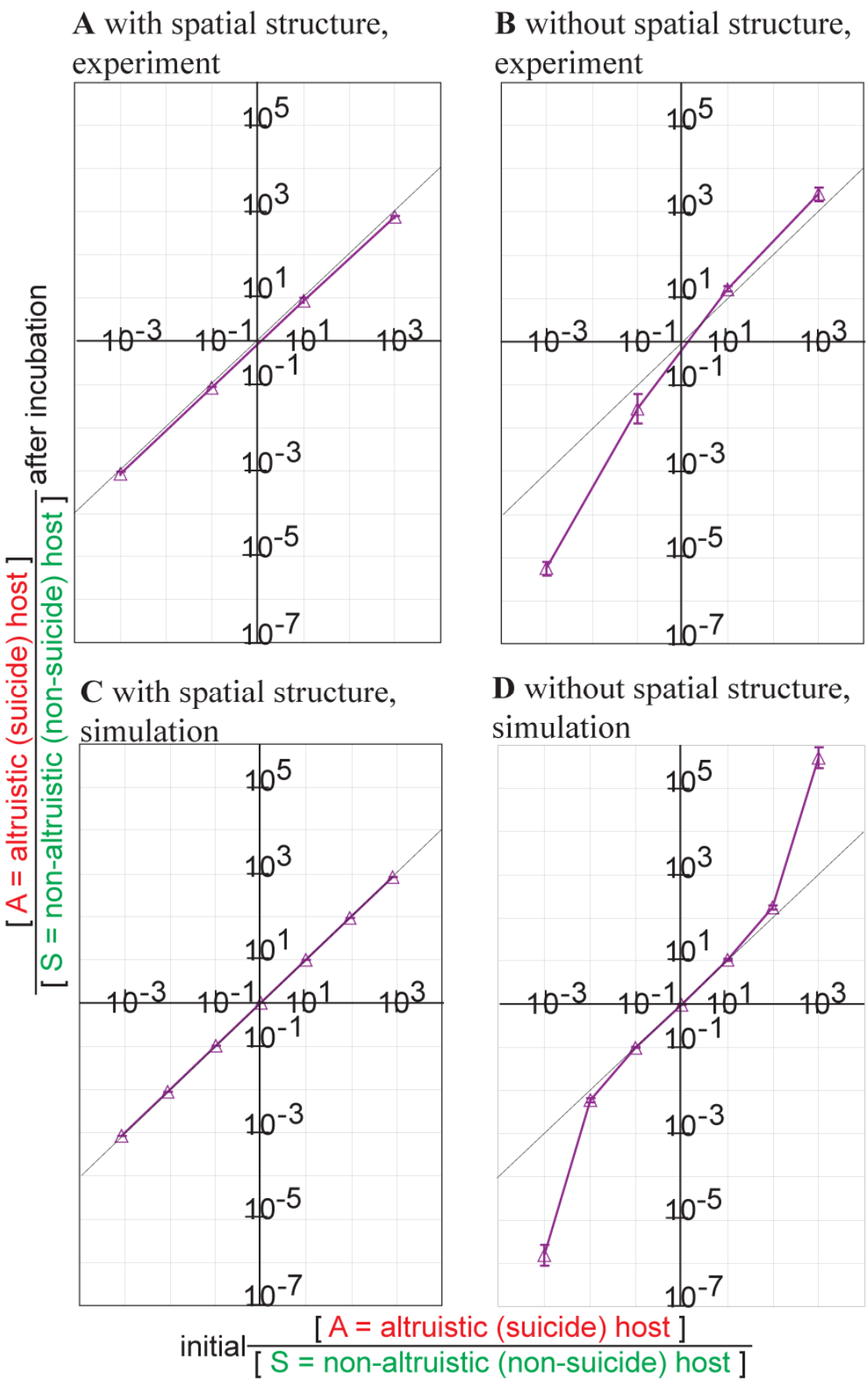
A with spatial structure, experiment
B without spatial structure, experiment
C with spatial structure, simulation
D without spatial structure, simulation
[A = altruistic (suicide) host] / [S = non-altruistic (non-suicide) host] after incubation
initial [A = altruistic (suicide) host] / [S = non-altruistic (non-suicide) host]
10^5
10^3
10^1
10^-1
10^-3
10^-5
10^-7
10^-3
10^-1
10^1
10^3

Figure 5. Changes of the A:S ratio with pathogen Q, which does not induce suicide in either host.

Final A:S ratio as a function of the initial A:S ratio. The averages ± SEM are shown. n = 4 for experiments and n = 100 for simulations.

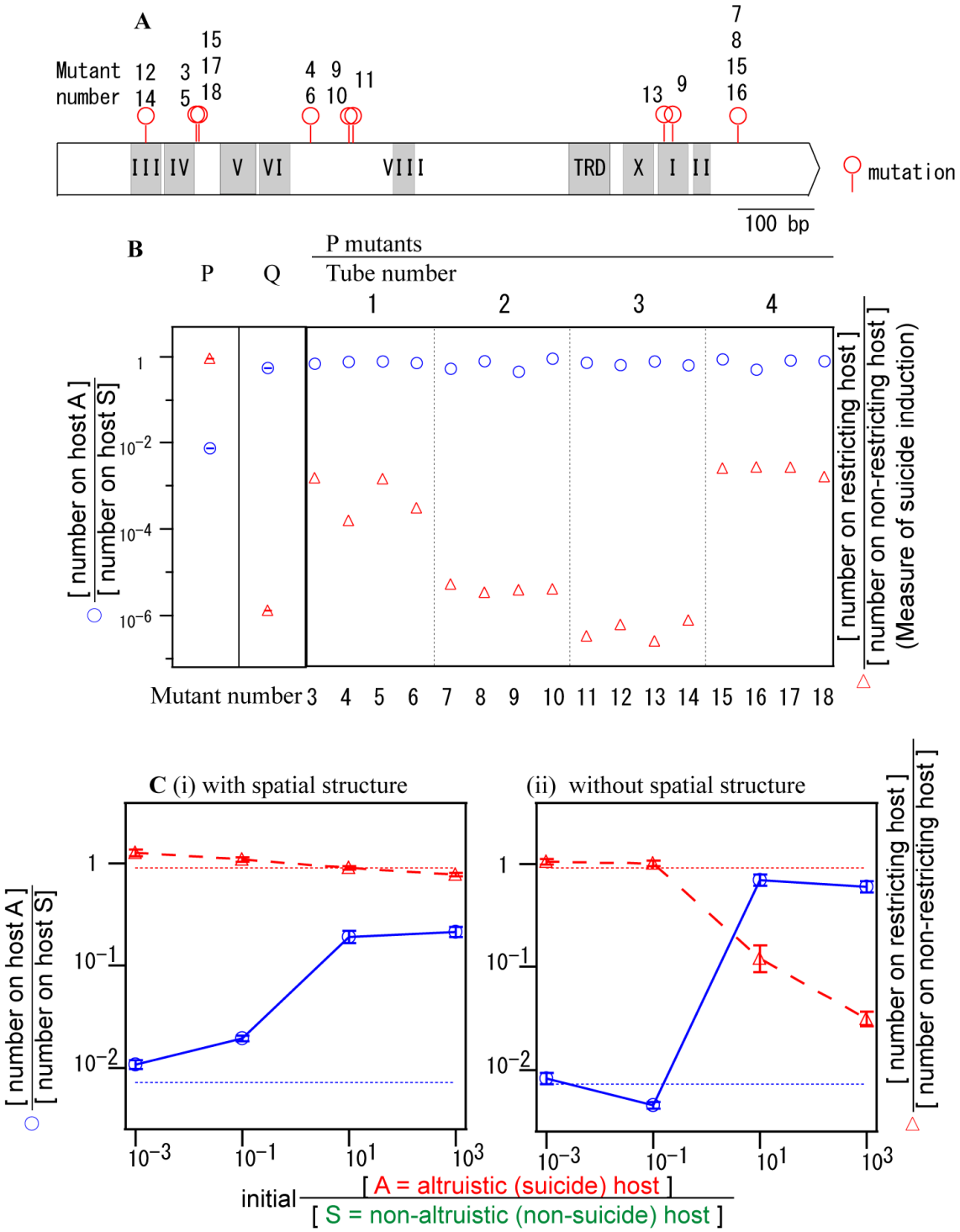
A
Mutant number
12 14
3 5
15 17 18
4 6
9 10
11
13
9
7 8 15 16
III IV V VI VIII TRD X I II
mutation
100 bp
B
P mutants
P Q
Tube number
1 2 3 4
[number on host A] / [number on host S]
[number on restricting host] / [number on non-restricting host]
(Measure of suicide induction)
Mutant number 3 4 5 6 7 8 9 10 11 12 13 14 15 16 17 18
C (i) with spatial structure
(ii) without spatial structure
[number on host A] / [number on host S]
[number on restricting host] / [number on non-restricting host]
initial [A = altruistic (suicide) host] / [S = non-altruistic (non-suicide) host]

Figure 6. Emergence of pathogen mutants defective in inducing host suicide. (*A*) Mutations in the DNA methyltransferase gene in mutants recovered after infection in the absence of spatial structure (initial A:S = 10^3). Roman numerals refer to motifs characteristic of DNA methyltransferases. See Table S3 for details of the mutants. (*B*) Characterization of the mutants. The ratio of the number measured in a restricting host ($PvuII^+$) to the number measured in a non-restricting host ($PvuII^-$) is a measure of defects in the pathogen's DNA methyltransferase (M.PvuII) activity, which induced suicide in host A. (*C*) Dependency of the mutant pathogen emergence on spatial structure and the initial host ratio.

Table 1. Pathogen mutants.

Tube number	Isolate number	Nucleotide position	Codon change	Amino acid change
1	3	186	AAA -> AAAa	K62frameshift
	4	371	GGT -> GtT	G124V
	5	186	AAA -> AAAa	K62frameshift
	6	371	GGT -> GtT	G124V
2	7	923	TTA -> T-A	L308frameshift
	8	923	TTA -> T-A	L308frameshift
	9	425	CCT -> CaT	P142H
	9	858	GAA -> GA-	E286frameshift
	10	425	CCT -> CaT	P142H
3	11	434	TGG -> TtG	W145L
	12	118	GAA -> tAA	E40stop
	13	823	GGC -> tGC	G275C
	14	118	GAA -> tAA	E40stop

4	15	187	GAA -> aGAA	E63frameshift
	15	923	TTA -> TT-	L308frameshift
	16	923	TTA -> TTtA	L308frameshift
	17	187	GAA -> aGAA	E63frameshift
	18	187	GAA -> aGAA	E63frameshift

K, Lysine; G, Glycine; V, Valine; L, Leucine; P, Proline; H, Histidine; E, Glutamic acid; W, Tryptophan; C, Cysteine.

Mathematical modeling and simulation

I conducted mathematical modeling and computer simulations using a large double-lattice with 10000 × 10000 cells in the presence of spatial structure and with a population of 10^8 in the absence of spatial structure (see Materials and methods for detail). My simulation (Fig. 3*C*, *D*) reproduced the essential features of my experimental results. Thus, in the presence of spatial structure, a pathogen increase was followed by an increase in the ratio of the two hosts (A:S) of two orders of magnitude. The essential features of my experimental results with other input ratios were also reproduced in the simulations (Fig. 3*G*, *H*).

In the absence of spatial structure, the pathogen increase was followed by a random (unpredictable) change in the A:S ratio (Fig. 3*D*). These changes were not biased in a large enough population (10^{10}), but they were biased towards decrease in a smaller population (10^8) (Fig. 7). I also observed the extinction (58/100) of host A at a population size of 10^8. Therefore, the decrease in the A:S ratio observed in the experiments (Fig. 3*F*, *H*) was probably due to limited population size, as discussed above. The host population members were replaced by mutants resistant to the pathogen (as described above). The smaller population could not initially harbor the resistant mutations, so there was a delay before their appearance. This explanation is consistent with the simulation and the experimental results. My detailed time course analysis treating A host density and S host density separately confirmed this interpretation (Fig. 8). The delay in acquiring a pathogen-resistant mutation apparently led to decrease in the A:S ratio (Fig. 8 *B*(*ii*)).

Fig. 4*C*, *D* show snapshots of a 100 × 100 area of the host lattice in the simulation

(see Supplemental animations for detail). The altruistic (suicidal) type host A (red) represents a minor (1/1000) proportion of the population (Fig. 4*C*). The non-altruistic (non-suicidal) host S (green) mediated a pandemic as indicated by the spread of the infected non-altruistic type host I (yellow). The altruistic host A (red) survived in a colony even when the neighboring non-altruistic host S colonies were eradicated during the pandemic. This resulted in a large increase in the A:S ratio after infection.

When the altruistic host A predominated in the population (Fig. 4*D*), a pandemic was not observed, because infection was prevented from spreading by the altruistic host A population surrounding the non-altruistic host S colony. This resulted in no great increase in the A:S ratio. This indicates that the altruistic host A could not eliminate the host S. An altruistic host allows neighboring altruistic and non-altruistic hosts to escape infection in a structured habitat. Thus, the altruistic host A is effectively parasitized by the freeloading S host.

Eemergence of the host mutants resistant to the pathogen was analyzed in Fig.9. And, my simulation reproduced features of pathogen mutants not inducing host suicide (Fig. 10). In the absence of spatial structure, both the host populations were replaced by pathogen-resistant mutants except for the case with largest A type host. In the last case, because of the suicidal defense by the A type host, the pathogen cannot increase in number to provide selective pressure. When host A (suicidal) is more than host S, the pathogen population is replaced by mutants that cannot induce host suicide. In the presence of spatial structure, I see similar trends but less extreme replacements. The S hosts were replaced by mutants when they formed the majority.

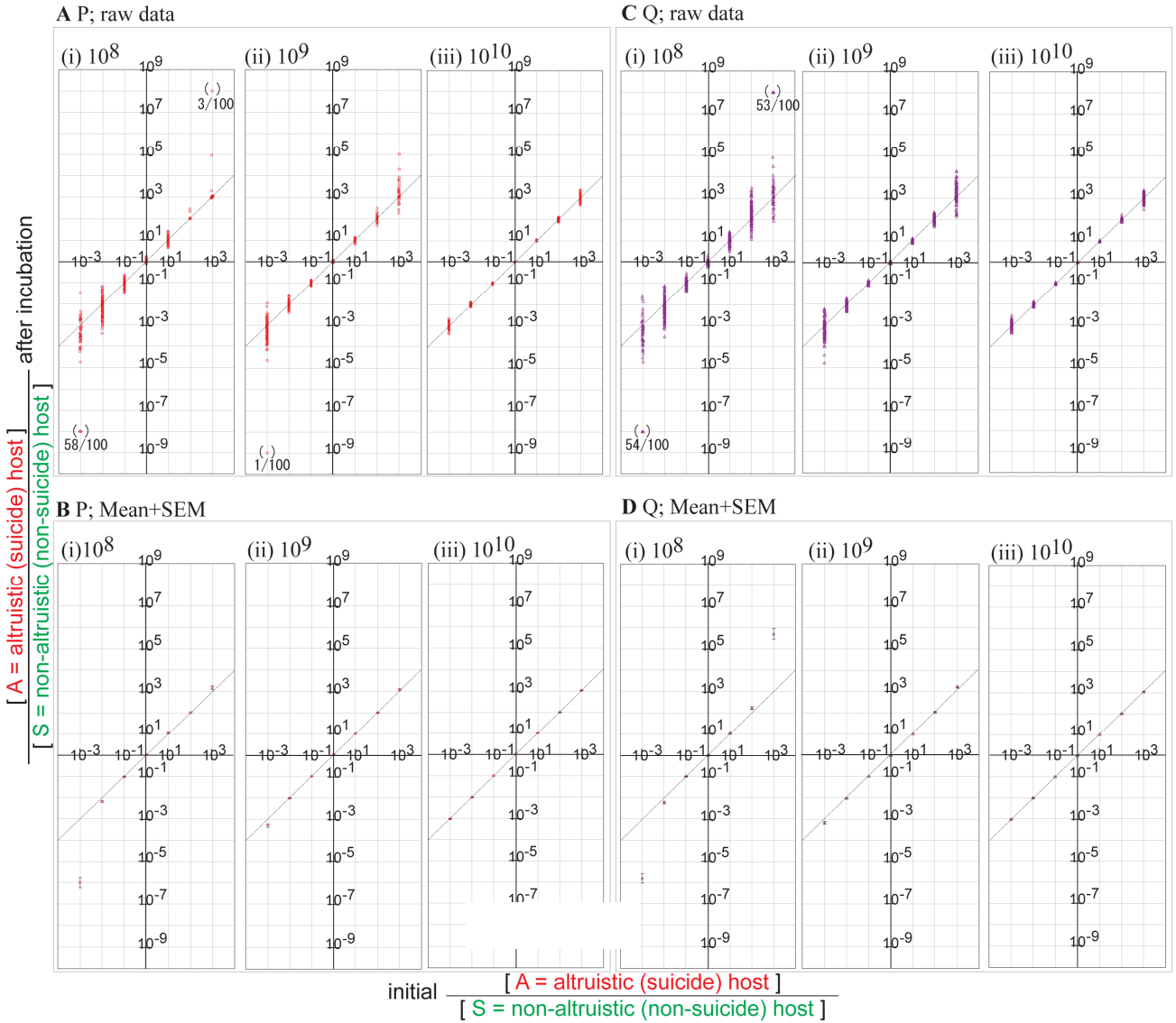
A P; raw data
C Q; raw data
B P; Mean+SEM
D Q; Mean+SEM
(i) 10^8
(ii) 10^9
(iii) 10^10
3/100
58/100
1/100
53/100
54/100
after incubation
[A = altruistic (suicide) host]
[S = non-altruistic (non-suicide) host]
initial
[A = altruistic (suicide) host]
[S = non-altruistic (non-suicide) host]

Figure 7. Effect of population size on the A:S ratio change in the absence of spatial structure.

Maximum population size was varied. With P pathogen (*A*, *B*) or Q pathogen (*C*, *D*). Individual results from simulations are shown for (*A*) and (*C*).

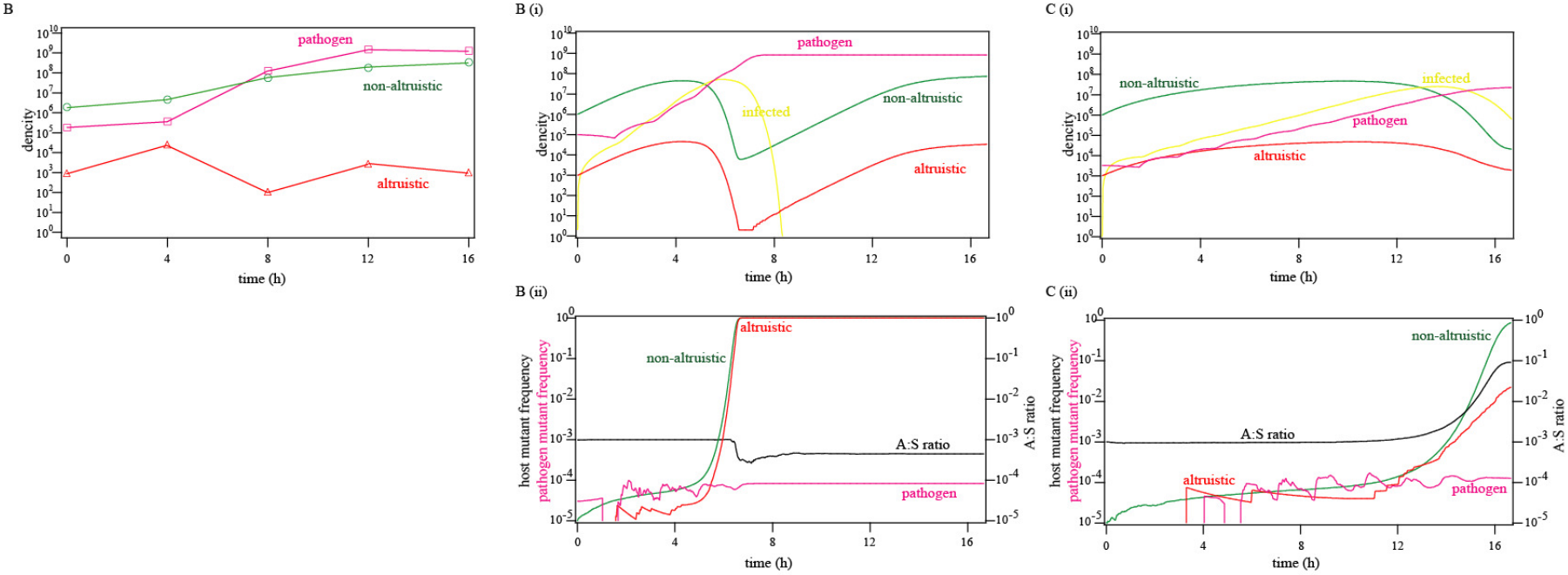
B
pathogen
non-altruistic
altruistic
density
time (h)
B (i)
pathogen
infected
non-altruistic
altruistic
density
time (h)
C (i)
non-altruistic
infected
pathogen
altruistic
density
time (h)
B (ii)
altruistic
non-altruistic
A:S ratio
pathogen
host mutant frequency
pathogen mutant frequency
A:S ratio
time (h)
C (ii)
non-altruistic
A:S ratio
altruistic
pathogen
host mutant frequency
pathogen mutant frequency
A:S ratio
time (h)

Figure 8. Detailed time-course analysis in the absence of spatial structure.

(*A*) Time-course of changes in hosts' densities and pathogen's density in an experiment without spatial structure. One out of four similar results. (*B(i)*) Time-course of changes in hosts' densities and pathogen's density in a simulation without spatial structure. (*B(ii)*) Mutant frequencies in the two hosts and A:S ratio in a simulation without spatial structure. (*C(i)*) Time-course of changes in hosts' densities and pathogen's density in a simulation with spatial structure. (*C(ii)*) Mutant frequencies in the two hosts and A:S ratio in a simulation with spatial structure. One out of 100 similar simulation results.

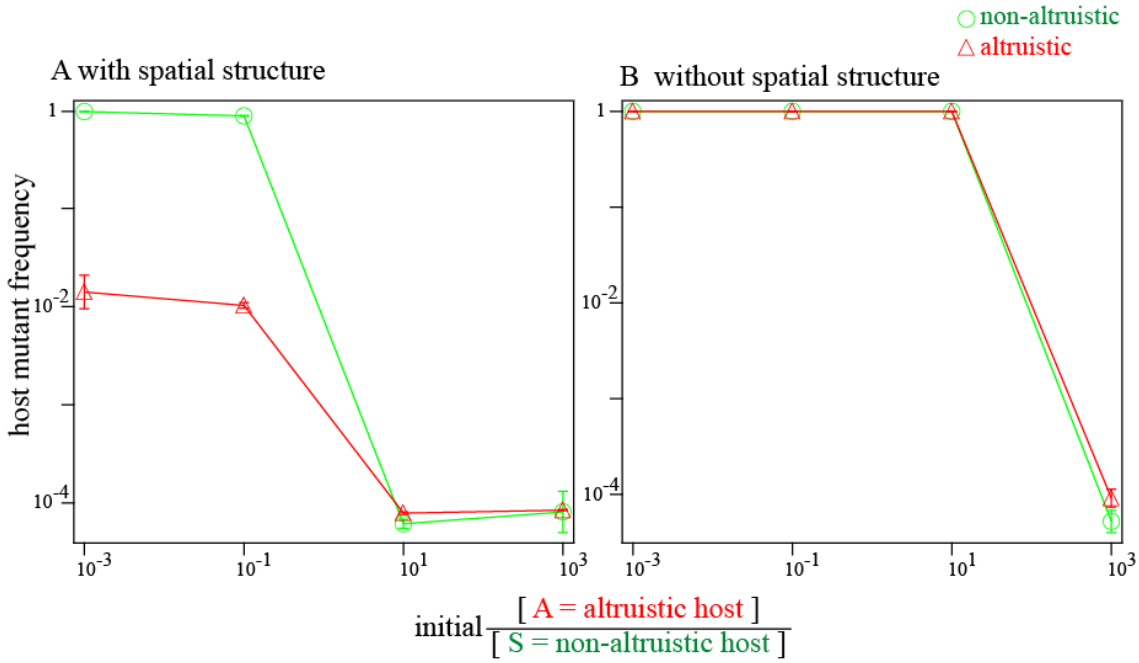

Figure 9. Dependency of the mutant host emergence on spatial structure and the initial host ratio in the simulation. (*A*) with spatial structure, (*B*) without spatial structure.

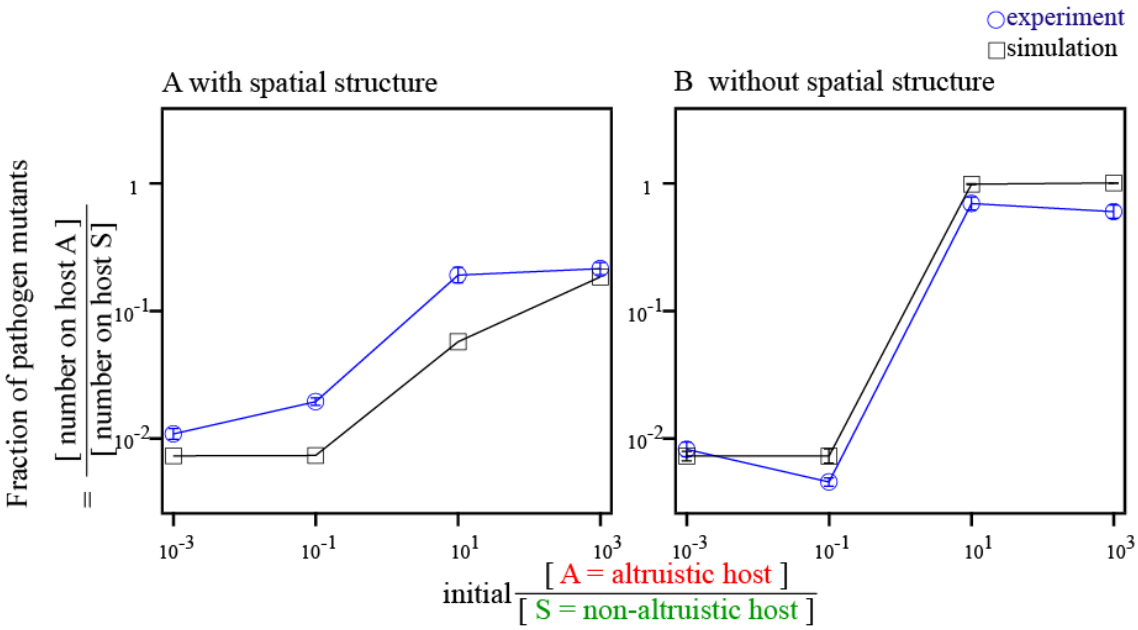

Figure 10. Dependency of the mutant pathogen emergence on spatial structure and the initial host ratio in the simulation. (*A*) with spatial structure, (*B*) without spatial structure.

I show how the fraction of mutants changes with time for the system without spatial structure for the simulation as Fig. 8b(ii). Pathogen increase (Fig. 8b(i)) was accompanied by increases in the host mutant frequency and a decrease in the A:S ratio. In the presence of spatial structure, infection proceeded slowly and led to pathogen increase at the last phase. This was accompanied by decrease of the type S host and increase of the pathogen resistant mutants.

Discussion

These results of infection experiments and simulation (Fig. 3) clearly indicate that a "Suicidal Defense Against Infection" (SDAI) strategy (Fig. 1; Fig. 2*A*) can evolve in the presence of spatial structure. In a simple example, the hosts in the internal part of an altruistic host colony would be protected by suicide of the individuals placed in its external part (Fig. 4). In the absence of spatial structure, however, altruistic hosts would be infected with pathogens from non-altruistic hosts, and non-altruistic hosts would also be protected by altruistic hosts. Spatial structure plays an important role in the kin selection-based theory of altruism(16). It is natural that spatial structure governs benefits of this extreme form of altruism based on kin selection.

The maximum benefit of SDAI strategy in the presence of spatial structure was obtained at the minimum initial A:S ratio (Fig. 3*E*). The higher the initial A:S ratio, the smaller the SDAI strategy benefit (Fig. 3*E*). Spread of infection among the non-altruistic hosts was presumably blocked by the surrounding altruistic hosts, when A:S ratio became larger. The SDAI strategy can invade the non-SDAI strategy and it is stable once established. However, it cannot eliminate the non-SDAI strategy. Such negative frequency dependence of altruist's fitness was expected from theory of social evolution

in structured populations with strong selection(17).

These results imply that virulence is a property, or function, of a host-pathogen interaction but not of a pathogen only. I revealed that the host strategy of inducing high virulence (or mortality) in the pathogen upon infection has the advantage of preventing pathogen spread. We realize a paradoxical competition between a host and a pathogen with respect to virulence and host induced virulence. Thus, if the pathogen favors less virulence to avoid host death and maintain sustainable symbiosis, the host favors more induced virulence to prevent the pathogen form spreading. Indeed, there was emergence of pathogen mutants defective in inducing suicide (less virulent mutants) under some conditions (Fig. 6). This is similar to arms race between pathogen infectivity and host resistance(8), which here led to emergence of host mutants resistant to the pathogen (Fig. 9).

Previous studies show that the presence of spatial structure can provide an advantage to less virulent pathogens(13). Under my two conditions, the fraction of less virulent mutants appeared lower in the presence of spatial structure (Fig. 10). However, these two conditions cannot be directly compared: selective pressure was weak in the presence of spatial structure due to the limited extent of infection.

Other examples of suicidal altruism in unicellular bacteria have been reported such as those accompanying production of bacteriocin(12) and stimulation of immune response(18). Suicidal defense against infection is seen in multi-cellular organisms at the level of cells, such as programmed death of infected mammalian and plant cells(19), and at the level of individuals, such as self-removal of infected individuals in social insects(20).

In this work, the unicellular bacterium *Escherichia coli* and bacteriophage

lambda, well studied for long time, were used as the model host and pathogen to study infection. However, my modeling took a general form not limited to pairs of bacteria and bacteriophage, so my experiment-simulation system will be useful for analysis of other forms of infection and biological interactions in general.

Materials and methods

Bacterial strains, bacteriophage strains, and plasmids

The *E. coli* K-12 strains, phages, and plasmids used are listed in Table 2. The non-artruistic type strain (BMF5, *mcrB::kan*, designated as S host in this study) was kanamycin-resistant and $lacZ^+$, whereas the altruistic type strain (BMF3, $mcrBC^+$, A host) was chloramphenicol-resistant and $lacZ^-$. McrBC is a methyl-specific DNase. Ciable counts (colony counts) can be selectively measured on agar plates containing kanamycin and agar plates containing chloramphenicol, so they can be differentially scored based on colony color on a special agar plate. The P pathogen that induced suicide in the S host was bacteriophage lambda carrying a gene for PvuII DNA methyltransferase, whereas the Q pathogen did not carry this gene. The lambda phage used in this work was int^- but cI^+. Therefore, stable lysogeny is impossible, but temporary immune state under some of the conditions cannot be excluded. However, presence of such temporary immunity, if any, does not affect my main conclusion that the altruistic host has advantage in the presence of spatial structure because presence of such temporary immunity should make the results with pathogen (P) closer to the results without pathogen. In my experiments in Figure 3(*E*), the altruistic host (red line) showed clear advantage over non-altruistic host with pathogen as opposed to the case without pathogen (olive line). I have not incorporated such temporary lysogeny into the

model, so I do not know whether it explains the difference between the experimental results and the simulation results.

A 0.7 kb fragment, including the *mrfp* or *gfpuv* gene, was amplified from pNG1(21) or pSHINE2121(22) using mRFP-1 (5′-CCagatctATGGCCTCCTCCGAGGACGTCAT-3′) and mRFP-2 (5′-GGgaattcTTAGGCGCCGGTGGAGTGGCGGC-3′) primers or GFPuv-1 (5′-CCagatctATGAGTAAAGGAGAAGAACTTTT-3′) and GFPuv-2 (5′-GGgaattcTTATTTGTAGAGCTCATCCATGC-3′) primers. Each PCR primer had an introduced restriction site, for BglII and EcoRI, at the 5′ end (small letters). The fragment was digested with BglII and EcoRI and inserted into pUC19 (laboratory collection) to generate pMF8 (pUC19-*mrfp*: Amp) or pMF9 (pUC19-*gfpuv*: Amp).

Table 2. Bacteria, phages and plasmids

Symbol	Bacterial strain	Genotype	Comments	Source and reference
	JC8679	F^- *thr-1 leuB-6 phi-1 lacY1 galK2 ara-14 xyl-5 mtl-1 proA2 his-4 argE3 rpsL31 tsx-33 supE44 recB21 recC22 sbcA23 his-328* λ^-		A. J. Clark, (22)
	JW5871	BW25113 *mcrB::kan*		National Institute of Genetics, (23)
	MG1655	F^- lambda$^-$ *ilvG*$^-$ *rfb*-50 *rph*-1		D. Biek, (24)
	BIK2146	JC8679 *lacZ::cml*		N. Handa, (25)
	BMF1	JC8679 *mcrB::kan*	P1 from JW5871 to JC8679	this work

A	BMF3	MG1655 *lacZ::cml*	P1 from BIK2146 to MG1655	this work
S	BMF5	MG1655 *mcrB::kan*	P1 from JW5871 to MG1655	this work
	BMF22	BMF3 carrying pMF8		this work
	BMF24	BMF5 carrying pMF8		this work
	BMF28	BMF5 carrying pMF9		this work
	BMF30	BMF3 carrying pMF9		this work
	BMF35	BMF5 carrying pYNEC323		this work
	BMF37	BMF5 carrying pYNEC324		this work

	Phage strain	Genotype	Source and reference
P	LEF1	Bam1^{0} ΔB *int*$^{-}$ *pvuIIM* Δ(*red-gam*)	E. Fukuda, (7)

		imm21 nin5 shn6^{0}		
Q	LIK891	Bam1^{0} ΔB *int*+ Δ(*red-gam*)	*imm21 nin5 shn6*^{0}	N. Handa, (26)
	λvir			A.Miura, (21)
	P1 vir			H. Ikeda, (27)

Plasmids	Relevant characteristics	Prototype plasmid	Drug resistance	Source and reference
pYNEC323	*pvuIIRMC cml*	pIK153	Cml	Y. Nakayama, (28)
pYNEC324	*pvuIIR⁻MC cml*	pIK153	Cml	Y. Nakayama, (28)
pMF8	*mrfp*	pUC19	Amp	this work
pMF9	*gfpuv*	pUC19	Amp	this work

kan, kanamycin-resistance gene; *cml*, chloramphenicol-resistance gene.

Growth medium

Host *E. coli* cells were grown in tryptone-maltose broth with 10 mM $MgSO_4$ (1.0% (w/v) tryptone, 0.5% (w/v) NaCl, 0.2% (w/v) maltose, and 10 mM $MgSO_4$). Antibiotics were added at the following concentrations as required: kanamycin (Kan) 20 μg mL^{-1} and chloramphenicol (Cml) 25 μg mL^{-1}.

Bacterial growth

Overnight cultures of hosts were diluted 100-fold and grown at 37 °C in Tryptone-maltose broth with 10 mM $MgSO_4$. When the cultures reached the mid-exponential phase, its cell concentration was adjusted to 10^8 cells mL^{-1} for storage at 4 °C.

Phage preparation and plaque assay

P1 vir was prepared on JC8679, and LEF1 was prepared on BMF1, using the plate lysate method(18). For the phage plaque assay, an overnight culture of *E. coli* was diluted 100-fold and grown to mid-exponential phase at 37 °C with aeration in tryptone-maltose broth with 10 mM $MgSO_4$. Phage was diluted appropriately and mixed with the culture. After incubation at room temperature for 10 min, the phage-bacteria complex was mixed with 2 mL of lambda polypeptone top agar (1.0% (w/v) polypeptone, 0.5% (w/v) NaCl, 0.2% maltose, 10 mM $MgSO_4$, and 0.6% Bactoagar) and poured on lambda polypeptone bottom agar (1.0% (w/v) polypeptone, 0.5% (w/v) NaCl, 0.2% maltose, 10 mM $MgSO_4$, and 1.0% Bactoagar) plate. Plates were incubated at 37 °C for 16 h and plaques were counted.

Infection

To investigate infection in the absence of spatial structure, the two hosts were mixed in various ratios with a total concentration of 10^7 cell mL^{-1} in 1 mL of tryptone-maltose broth with 10 mM $MgSO_4$. I then added 10^6 plaque-forming units of the pathogen. After 10 min of incubation at room temperature, 2 mL of tryptone-maltose broth was added and the tubes were incubated in an orbital shaker for 16 h at 37 °C. Samples were taken from this culture, and the count of the non-altruistic host S was determined on LB agar containing 20 μg mL^{-1} kanamycin, while the altruistic-type host A count was determined on LB with 25 μg mL^{-1} chloramphenicol. The phage titer (the number of viable pathogens) was assayed on *E. coli* BMF1.

To investigate infection in the presence of spatial structure, the host and the pathogen were grown in a soft agar matrix spread over a bottom agar plate. To initiate the soft agar culture, 10^4 to 10^7 cells of each type of host were mixed in various ratios (a total of 10^7 cells) and 10^6 plaque-forming units of phages were added to 1 mL of tryptone-maltose broth with 10 mM $MgSO_4$. Ten minutes of incubation were allowed for adsorption, before 2 mL of molten (50 °C) top agar (tryptone-maltose broth with 10 mM $MgSO_4$ and 0.6% agar) was added. The suspension was then poured onto Petri plates containing about 30 ml of hardened bottom agar (tryptone-maltose broth with 10 mM $MgSO_4$ and 1.0% agar). After an incubation period of 0 to 16 h at 37 °C, the soft agar matrix was scraped off into a tube containing 1 mL of tryptone broth (without maltose and agar) and vortexed for 30 sec to liberate the host and pathogen from the soft agar, before the agar fragments were separated by centrifugation at 1600 g for 2 min at 4 °C. The counts of the pathogen and the ratio of the two hosts were measured as above.

Fluorescent microscopy

Fluorescent microscopic imaging was used in the presence of spatial structure, where the host and the pathogen were grown in a covered soft agar matrix spread over a bottom agar plate. To initiate the soft agar culture, 10^6 to 10^7 cells of each type host in various ratios (a total of 10^7 cells), and 10^6 plaque-forming units of the phage, were added to 1 mL of tryptone-maltose broth containing 10 mM $MgSO_4$ and 10 μg mL^{-1} ampicillin. After 10 min of incubation to allow adsorption at room temperature, 2 mL of molten (50 °C) soft agar (tryptone broth with 0.6% agar) was added. Then, 0.6 mL of the soft agar suspension was poured onto a Petri plate containing about 30 mL of hardened bottom agar (tryptone-maltose broth with 10 mM $MgSO_4$, 1.0% agar, and 10 μg mL^{-1} ampicillin). After 10 min of cooling at 4 °C, 0.6 mL of molten (50 °C) soft agar (tryptone broth with 0.6% agar) was poured over to produce an overlay of top agar. After incubation for 16 h at 37 °C, the plates were stored at 4 °C.

mRFP fluorescence was imaged with 510–560 nm excitation, a 590 nm emission filter, and a 575 nm diachroic mirror. GFPuv fluorescence was imaged with 465–495 nm excitation, a 515–555 nm emission filter, and a 505 nm diachroic mirror.

Identification and characterization of mutants

Host mutants resistant to pathogen were detected as colony formers on polypeptone agar plates (1.0% (w/v) polypeptone, 0.5% (w/v) NaCl, 0.2% maltose, 10 mM $MgSO_4$, and 1.3% Bactoagar) seeded with 10^9 plaque-forming units of $lambda_{vir}$. If the colony-forming units on a plate were similar to that on tryptone agar plate without $lambda_{vir}$, the bacterium was defined as resistant. Otherwise, they were judged as sensitive.

A *pvuIIM*$^-$ mutant of the pathogen was determined by plaque assay. When the

pathogen titer on the altruistic host was similar to that of the non-altruistic host, it was judged as *pvuIIM*$^{-}$. Otherwise, it was judged as *pvuIIM*$^{+}$. The ratio of the number measured in a restricting host (R.PvuII^{+}, BMF35) to the number measured in a non-restricting host (R.PvuII^{-}, BMF37) was a measure of defects in the pathogen's methyltransferase (M.PvuII) activity.

Sequence determination

The phage suspensions were prepared from a single plaque in 0.1 mL of 0.1 M NaCl, 5 mM $MgSO_4$, 50 mM Tris-HCl, and 0.01% gelatin (SM buffer). A 5.1 kb fragment containing the *pvuIIM* gene was amplified by PCR using the primer LEF1-for (5′-TGTTTTACCACACCCATTCC-3′) and LEF1-rev (5′-ATCCCCATTCTGCAATGTGCG-3′). The temperature cycling in a program temperature control system (ASTEC) was as follows: 10 s at 98 °C, 15 s at 55 °C, and 5 min 10 s at 72 °C for 30 cycles. I determined the sequences using the primers PvuIIM_pcr-for (5′-TTAGCTCTTCAGGCTTCTGA-3′), PvuIIM_seq-rev (5′-CGGCTAAACTCGATAGAACA-3′), Primer 2 (5′-GGGGCGTACATGAAAGGCGT-3′), and Primer 5 (5′-CTCGGGTAACTTAGCAGGA-3′).

Model

Definitions of variables, parameters, and terms are summarized in Table 3. I embedded my virtual host-pathogen community in two layers of lattice, each composed of 10000 × 10000 regular squares (Fig. 11). The upper lattice contained the host population, where each square was either empty or occupied by: a susceptible host (S:

non-altruistic type), a resistant susceptible host (S^R: mutant form of S, resistant to any type of pathogen), an infected host (I: infected form of S by P), an infected host (I^Q: infected form of S or A by Q), an altruistic host (A: suicide type), a resistant altruistic host (A^R: mutant form of A, resistant to any type of pathogen) (Fig. 11). The lower lattice contained the pathogen population, where each square was either empty or occupied by pathogens (P: induces suicide in S host) or mutant pathogens (Q: mutant defective in induction of host suicide) (Fig. 11).

With spatial structure, the reproduction of S (S^R, A, or A^R) filled a neighboring empty site at a rate of $(1-\mu)r/4$ (Fig. 11*A*). Mutational reproduction of S (or A) filled a neighboring empty site at a rate of $r\mu/4$ (Fig. 11*B*). P (or Q) infection of S (or A) occurred in the upper site and neighboring sites at a rate of $(1-\mu)\beta/5$ (Fig. 11*C*, *D*). P infection was associated with P to Q mutation, and occurred in S (or A) in the upper site and neighboring sites at a rate of $\mu\beta/5$ (Fig. 11*E*). The death of I was accompanied by P release to the lower site after τ min from infection (Fig. 11*G*). P (or Q) was absorbed by S (I or A) in the upper site and neighboring sites at a rate of $a/5$ (Fig. 11*F*).

When spatial structure was absent, host reproduction, pathogen infection, and adsorption occurred at any site.

Details of the model are described in the appendix.

Table 3. Symbols.

Symbol	Definition
Host	
S	Susceptible; Non-suicide type
A	Altruistic; Suicide type
I	Infected form of S by P
S^R	Mutant form of S resistant to pathogen
A^R	Mutant form of A resistant to pathogen
I^Q	Infected form of S by Q
Pathogen	
P	Induces suicide in S host
Q	Mutant defective in induction of suicide
Host lattice	
O-site	Empty
S-site	Occupied by susceptible host

S^R-site	Occupied by resistant susceptible host
I-site	Occupied by infected host
I^Q-site	Occupied by mutant infected host
A-site	Occupied by altruistic host
A^R-site	Occupied by resistant altruistic host

Pathogen lattice

O-site	Empty
P-site	Occupied by pathogen
Q-site	Occupied by mutant pathogen

invariable		Value
z_r	Number of nearest-neighbors for reproduction	4
Z_d	Number of d (=7) step neighbor sites for infection and adsorption	113
r	Growth rate of host	0.023 min^{-1}
β	Infection rate of pathogen	47.5 s^{-1}
τ	Lysis time of infected host	60 min (30)
μ	Mutaion rate of host and pathogen	1.00E-5

a	Adsorption rate of lambda phage	1.58 s^{-1}
d	Infection radius	7
b	Burst size of pathogen	30 (29)

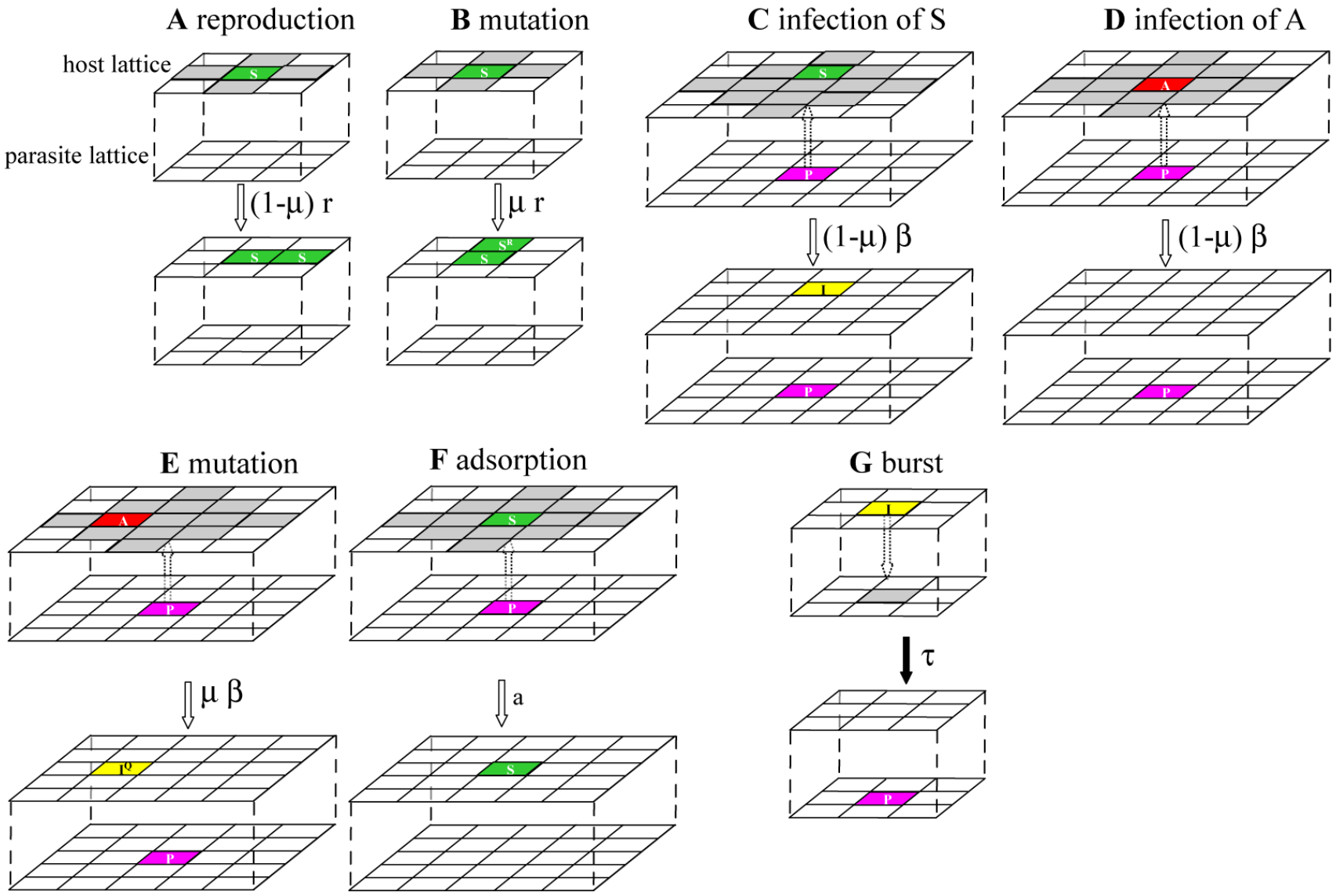
A reproduction
B mutation
C infection of S
D infection of A
host lattice
parasite lattice
(1-μ) r
μ r
(1-μ) β
(1-μ) β
E mutation
F adsorption
G burst
μ β
a
τ
S
A
P
I
S^R
I^Q

Figure 11. Model of the simulation with spatial structure.

(*A*) Reproduction of host S (or S^R, A and A^R). (*B*) Mutation of host S to S^R. Mutation of A to A^R. (*C*) Infection of host S with pathogen P (or Q). (*D*) Suicide of host A induced by infection with pathogen P. (*E*) Mutation of pathogen P to Q. (*F*) Adsorption of pathogen P (or Q) to S (or I, I^Q and A). (*G*) Death of host I (or I^Q) accompanied by release of pathogen P (or Q) τ min after infection.

References

1. Ebert, D & Mangin, KL (1997)The influence of host demography on the evolution of virulence of a microsporidian gut parasite. *Evolution* **51**, 1828-1837.

2. May, RM & Anderson, RM (1983)Epidemiology and Genetics in the Coevolution of Parasites and Hosts. *Proceedings of the Royal Society of London Series B-Biological Sciences* **219**, 281-313.

3. May, RM & Nowak, MA (1994)Superinfection, Metapopulation Dynamics, and the Evolution of Diversity. *Journal of Theoretical Biology* **170**, 95-114.

4. Weinrauch, Y & Zychlinsky, A (1999)The induction of apoptosis by bacterial pathogens. *Annu Rev Microbiol* **53**, 155-87.

5. Belser, J. A. et al. (2008)Contemporary North American influenza H7 viruses possess human receptor specificity: Implications for virus transmissibility. *e* **105**, 7558-7563.

6. Chopin, MC, Chopin, A & Bidnenko, E (2005)Phage abortive infection in lactococci: variations on a theme. *Current Opinion in Microbiology* **8**, 473-479.

7. Fukuda, E, Kaminska, KH, Bujnicki, JM & Kobayashi, I (2008)Cell death upon epigenetic genome methylation: a novel function of methyl-specific deoxyribonucleases. *Genome Biology* **9**.

8. Brockhurst, MA, Buckling, A & Rainey, PB (2006)Spatial heterogeneity and the stability of host-parasite coexistence. *Journal of Evolutionary Biology* **19**, 374-379.

9. Haraguchi, Y & Sasaki, A (2000)The evolution of parasite virulence and transmission rate in a spatially structured population. *Journal of Theoretical Biology* **203**, 85-96.

10. Kamo, M, Sasaki, A & Boots, M (2007)The role of trade-off shapes in the evolution of parasites in spatial host populations: An approximate analytical approach. *Journal of Theoretical Biology* **244**, 588-596.

11. Sato, K, Matsuda, H & Sasaki, A (1994)Pathogen Invasion and Host Extinction in Lattice Structured Populations. *Journal of Mathematical Biology* **32**, 251-268.

12. Chao, L & Levin, BR (1981)Structured Habitats and the Evolution of Anticompetitor Toxins in Bacteria. *Proceedings of the National Academy of Sciences of the United States of America-Biological Sciences* **78**, 6324-6328.

13. Kerr, B, Riley, MA, Feldman, MW & Bohannan, BJM (2002)Local dispersal promotes biodiversity in a real-life game of rock-paper-scissors. *Nature* **418**, 171-174.

14. Mochizuki, A, Yahara, K, Kobayashi, I & Iwasa, Y (2006)Genetic addiction: selfish gene's strategy for symbiosis in the genome. *Genetics* **172**, 1309-1323.

15. Schrag, SJ & Mittler, JE (1996)Host-parasite coexistence: The role of spatial refuges

in stabilizing bacteria-phage interactions. *American Naturalist* **148**, 348-377.

16 Griffin, A. S. & West, S. A. Kin selection: fact and fiction. *Trends in Ecology & Evolution* **17**, 15-21 (2002).

17 Ross-Gillespie, A., Gardner, A., West, S. A. & Griffin, A. S. Frequency dependence and cooperation: theory and a test with bacteria. *American Naturalist* **170**, 331-342 (2007).

18 Ackermann, M. et al. Self-destructive cooperation mediated by phenotypic noise. *Nature* **454**, 987-990 (2008).

19 Rueppell, O., Hayworth, M. K. & Ross, N. P. Altruistic self-removal of health-compromised honey bee workers from their hive. *Journal of Evolutionary Biology* **23**, 1538-1546 (2010).

20 James, E. R. & Green, D. R. Infection and the origins of apoptosis. *Cell Death and Differentiation* **9**, 355-357 (2002).

21. Handa, N., Amitani, I., Gumlaw, N., Sandler, S. J. & Kowalczykowski, S. C. Single Molecule Analysis of a Red Fluorescent RecA Protein Reveals a Defect in Nucleoprotein Filament Nucleation That Relates to Its Reduced Biological Functions. *Journal of Biological Chemistry* **284**, 18664-18673 (2009).

22. Ohashi, Y., Ohshima, H., Tsuge, K. & Itaya, M. Far different levels of gene

expression provided by an oriented cloning system in *Bacillus subtilis* and Escherichia coli. *Fems Microbiology Letters* **221**, 125-130 (2003).

23. Hendrix, R. W., Roberts, J. W., Stahl, F. W. & Weisberg, R. A. lambda II (Cold Spring Harbor Laboratory, 1983).

24. Gillen, J. R., Willis, D. K. & Clark, A. J. Genetic-Analysis of the Rece Pathway of Genetic-Recombination in *Escherichia-Coli* K-12. *Journal of Bacteriology* **145**, 521-532 (1981).

25. Baba, T. et al. Construction of *Escherichia coli* K-12 in-frame, single-gene knockout mutants: the Keio collection. *Mol Syst Biol* **2**, 2006 0008 (2006).

26. Blattner, F. R. et al. The complete genome sequence of *Escherichia coli* K-12. *Science* **277**, 1453-& (1997).

27. Handa, N., Nakayama, Y., Sadykov, M. & Kobayashi, I. Experimental genome evolution: large-scale genome rearrangements associated with resistance to replacement of a chromosomal restriction-modification gene complex. *Molecular Microbiology* **40**, 932-940 (2001).

28. Handa, N., Ohashi, S., Kusano, K. & Kobayashi, I. chi*, a chi-related 11-mer sequence partially active in an *E-coli* recC* strain. *Genes to Cells* **2**, 525-536 (1997).

29. Lobocka, M. B. et al. Genome of bacteriophage P1. *Journal of Bacteriology* **186**, 7032-7068 (2004).

30. Nakayama, Y. & Kobayashi, I. Restriction-modification gene complexes as selfish gene entities: Roles of a regulatory system in their establishment, maintenance, and apoptotic mutual exclusion. *Proceedings of the National Academy of Sciences of the United States of America* **95**, 6442-6447 (1998).

31. Shao, Y. P. & Wang, I. N. Bacteriophage adsorption rate and optimal lysis time. *Genetics* **180**, 471-482 (2008).

32. Gadagkar, R. & Gopinathan, K. P. Bacteriophage burst size during multiple infections. *Journal of Biosciences* **2**, 253-259 (1980).

33. Nagashima, A. Viscosity of Water Substance - New International Formulation and Its Background. *Journal of Physical and Chemical Reference Data* **6**, 1133-1166 (1977).

Acknowledgments

This work was carried out under supervision by Professor Ichizo Kobayashi in collaboration with Dr. Akira Sasaki (Sokendai).

I am grateful to Dr. Ichizo Kobayashi for guidance, helpful discussion and critical reading of this thesis. I thank Dr. Akira Sasaki for guiding me in simulation. I thank Dr. Naofumi Handa, Dr. Noriko Takahashi, Dr. Mikihiko Kawai, Mr. Takeshi Tsuru, and Dr. Yoshikazu Furuta for helpful discussion and comments.

Computation was carried out in the Super Computer System, Human Genome Center, Institute of Medical Science, University of Tokyo.

Appendix

Detailed model

I modeled my virtual populations in a 10000×10000 dual-lattice (Fig. 11). One lattice was for the host, while the other was for the pathogen. I assume that each grid of the lattice has a side length $1\mu m$, and that each grid can harbor only one bacteria cell (whose diameter is about 0.5 μm). The state of the *i*th site ($i = 1,2,\cdots$) in the host lattice at time t is denoted by $s_i^{\mathrm{h}}(t) \in \Sigma^{\mathrm{h}} \equiv \left\{\mathrm{S},\mathrm{S}^{\mathrm{R}},\mathrm{A},\mathrm{A}^{\mathrm{R}},\mathrm{I},\mathrm{I}^{\mathrm{Q}},\mathrm{O}\right\}$ (Table 3). The state S indicates the site occupied by a sensitive non-altruistic (non-suicidal) host, S^{R} does the site occupied by a pathogen-resistant non-altruistic (non-suicidal) host, A does the site occupied by an altruistic (suicidal) host, A^{R} does the site occupied by a pathogen-resistant altruistic (suicidal) host, I does the site occupied by an infected host, I^{Q} does the site occupied by a host infected with a mutant pathogen, while O is an empty site. The state of the *i*th site ($i = 1,2,\cdots$) in the pathogen lattice at time *t* is denoted $s_i^{\mathrm{p}}(t) \in \Sigma^{\mathrm{p}} \equiv \left\{\mathrm{P},\mathrm{Q},\mathrm{O}\right\}$. The state P indicates that the site is occupied by *b* (burst size) individual pathogens, Q indicates that the site is occupied by *b* of individual mutant pathogens, while O is an empty site. The state of the whole lattice population at time *t* is expressed by a vector $\mathrm{W}(t) = ((s_1^{\mathrm{h}}(t), s_1^{\mathrm{p}}(t)),(s_2^{\mathrm{h}}(t), s_2^{\mathrm{p}}(t)),\cdots)$.

Assuming a continuous-time Markov process, I specify the dynamics of W(*t*) by

the following transition rates at the *i*th site (i = 1, 2, ...):

$(\mathrm{O},{*}\mathrm{p}) \to (\mathrm{S},{*}\mathrm{p}),(\mathrm{A},{*}\mathrm{p})$ at rate $r(1-\mu)n_i(\mathrm{S})/z_r$, and $r(1-\mu)n_i(\mathrm{A})/z_r$, (1)

$(\mathrm{O},{*}\mathrm{p}) \to (\mathrm{S}^{\mathrm{R}},{*}\mathrm{p}),(\mathrm{A}^{\mathrm{R}},{*}\mathrm{p})$ at rate $r\mu n_i(\mathrm{S})/z_r + rn_i(\mathrm{S}^{\mathrm{R}})/z_r$,

and $r\mu n_i(\mathrm{A})/z_r + rn_i(\mathrm{A}^{\mathrm{R}})/z_r$, (2)

$(\mathrm{S},{*}\mathrm{p}) \to (\mathrm{I},{*}\mathrm{p})$ at rate $\beta(1-\mu)m_i^{\mathrm{p}}(\mathrm{P})/Z_d$, (3)

$(\mathrm{A},{*}\mathrm{p}) \to (\mathrm{O},{*}\mathrm{p})$ at rate $\beta(1-\mu)m_i^{\mathrm{p}}(\mathrm{P})/Z_d$, (4)

$(\mathrm{S},{*}\mathrm{p}),(\mathrm{A},{*}\mathrm{p}) \to (\mathrm{I}^{\mathrm{Q}},{*}\mathrm{p})$ at rate $\beta\mu m_i^{\mathrm{p}}(\mathrm{P})/Z_d + \beta m_i^{\mathrm{p}}(\mathrm{Q})/Z_d$, (5)

$(\mathrm{I},{*}\mathrm{p}) \to (\mathrm{O},\mathrm{P})$ after lysis time τ, (6)

$({*}\mathrm{h},\mathrm{P}) \to ({*}\mathrm{h},\mathrm{O})$ at rate $a(m_i^{\mathrm{h}}(\mathrm{S}) + m_i^{\mathrm{h}}(\mathrm{I}) + m_i^{\mathrm{h}}(\mathrm{A}))/Z_d$, (7)

where the variable $n_i(\mathrm{s}^{\mathrm{h}})$ is the number of sites with state s^{h} in the nearest-neighbors of the *i*th site of the host lattice, $m_i^{\mathrm{p}}(\mathrm{s}^{\mathrm{p}})$ is the number of sites with state s^{p} in the d step neighbors of the *i*th site of the pathogen lattice (that is, the sites that are no further than d Manhattan distance, the sum of vertical and horizontal moves, from the *i*th site), $m_i^{\mathrm{h}}(\mathrm{s}^{\mathrm{h}})$ is the number of sites with state s^{h} in the *i*th site and the d step neighbors of the *i*th site of the host lattice. The constant $z_r = 4$ is the number of nearest neighbors of a site for host reproduction, and the constant $Z_d = 1 + 2d(d+1)$ is the number of d step neighbor sites for pathogen infection and adsorption. The character $*\mathrm{p}$ is a wildcard state that can be replaced by any state from Σ^{p}, while $*\mathrm{h}$ is a

wildcard state that can be replaced by any state from Σ^h.

Process (1) represents the reproduction of a sensitive non-altruistic host and an altruistic host to an empty site from a nearest-neighbor site on the host lattice, where μ is a constant parameter representing mutation rate, and r is a constant parameter representing maximum fecundity of a sensitive non-altruistic host and an altruistic host, which is implemented when all nearest-neighbor sites in the host lattice are empty.

Process (2) represents the mutational-reproduction of a sensitive non-altruistic host and an altruistic host, and the reproduction of a resistant non-altruistic host and a resistant altruistic host to an empty site from a nearest-neighbor site in the host lattice.

Process (3) represents the infection of a sensitive non-altruistic host at the *i*th site by a pathogen in its d step neighbors, where β is a constant parameter representing the maximum productivity of pathogens, which is implemented when all the d step neighbor sites are occupied by sensitive non-altruistic hosts.

Process (4) also represents the infection of an altruistic host at the *i*th site by a pathogen in its d step neighbors.

Process (5) represents the mutational-transmission of a pathogen and transmission of a mutant pathogen to a host at the *i*th site from its d step neighbors.

Process (6) represents the lysis process of an infected non-altruistic host, where

τ is a constant parameter representing lysis time.

Process (7) represents the adsorption of *b* individual pathogens at the *i*th site by a host in its d step neighbors, where $a(=\beta / b)$ is a constant parameter representing the maximum consumption of pathogens, which is implemented when all the d step neighbor sites are occupied by non-resistant hosts in the host lattice.

I refer to the variables $n_i(\mathrm{s}^{\mathrm{h}}) / z_r$, $m_i^{\mathrm{p}}(\mathrm{s}^{\mathrm{p}}) / Z_d$, and $m_i^{\mathrm{h}}(s^{\mathrm{h}}) / Z_d$ as "local density", which is used in the case of local interaction. In the case of global interaction, I refer to "global density" $\rho^{\mathrm{h}}(\mathrm{s}^{\mathrm{h}})$ and $\rho^{\mathrm{p}}(\mathrm{s}^{\mathrm{p}})$ instead.

$(\mathrm{O},*\mathrm{p}) \to (\mathrm{S},*\mathrm{p}),(\mathrm{A},*\mathrm{p})$ at rate $r(1-\mu)\rho^{\mathrm{h}}(\mathrm{S})$, and $r(1-\mu)\rho^{\mathrm{h}}(\mathrm{A})$, (1)'

$(\mathrm{O},*\mathrm{p}) \to (\mathrm{S}^{\mathrm{R}},*\mathrm{p}),(\mathrm{A}^{\mathrm{R}},*\mathrm{p})$ at rate $r\mu\rho^{\mathrm{h}}(\mathrm{S}) + r\rho^{\mathrm{h}}(\mathrm{S}^{\mathrm{R}})$,

and $r\mu\rho^{\mathrm{h}}(\mathrm{A}) + r\rho^{\mathrm{h}}(\mathrm{A}^{\mathrm{R}})$, (2)'

$(\mathrm{S},*\mathrm{p}) \to (\mathrm{I},*\mathrm{p})$ at rate $\beta(1-\mu)\rho^{\mathrm{p}}(\mathrm{P})$, (3)'

$(\mathrm{A},*\mathrm{p}) \to (\mathrm{O},*\mathrm{p})$ at rate $\beta(1-\mu)\rho^{\mathrm{p}}(\mathrm{P})\beta\ (1 - \mu)\ \rho^{p}(\mathrm{P})$, (4)'

$(\mathrm{S},*\mathrm{p}),(\mathrm{A},*\mathrm{p}) \to (\mathrm{I}^{\mathrm{Q}},*\mathrm{p})$ at rate $\beta\mu\rho^{\mathrm{p}}(\mathrm{P}) + \beta\rho^{\mathrm{p}}(\mathrm{Q})$, (5)'

$(*\mathrm{h},\mathrm{P}) \to (*\mathrm{h},\mathrm{O})$ at rate $a(\rho^{\mathrm{h}}(\mathrm{S}) + \rho^{\mathrm{h}}(\mathrm{I}) + \rho^{\mathrm{h}}(\mathrm{A}))$, (7)'

where $\rho^{\mathrm{h}}(\mathrm{s}^{\mathrm{h}})$ is the number of sites with state s^{h} in the host lattice divided by the lattice size, and $\rho^{\mathrm{p}}(\mathrm{s}^{\mathrm{p}})$ is the number of sites with state s^{p} in the pathogen lattice divided by the lattice size.

To initialize the simulation, every host lattice site was randomly and independently assigned one of the state in $\Sigma^{h} \equiv \left\{S, S^{R}, A, A^{R}, I, I^{Q}, O\right\}$, and every pathogen lattice site was assigned as O. In the case of global interaction, each host is on a host lattice site, but it can interact with a pathogen wherever it is on the pathogen lattice. In the case of local interaction, each host can interact only with a pathogen in the nearest-neighbor site and its own site. Simulations were repeated 100 times for each condition.

The diffusion coefficient for phage, *D*, is described using the Stokes-Einstein relation:

$$D = \frac{k_{B} T}{6\pi\eta R}, \tag{8}$$

where *R* is approximately the radius of the phage head, and η is the viscosity of the medium, *T* is absolute temperature, and k_{B} is the Boltzmann constant. The maximum adsorption rate *k* corresponds to the case of total cell absorption, where the surface of the cell is entirely covered by receptors:

$$k = 4\pi c D, \tag{9}$$

where *c* is the cell radius. From equation (8) and (9), I calculated *k* = 47.5 μm^{3} s^{-1} when *R* = 30 nm, *T* = 37 °C = 310 K, η = 0.01 P = 0.01 g cm^{-1} s^{-1}(33), *c* = 0.5 μm, and k_{B} = 1.38 × 10^{-23} m^{2} kg s^{-2} K^{-1}. I approximated *k* as the infection rate of the pathogen.

After b phage particles are released at time $t=0$ at the origin, the concentration of the phage, *C*, would obey the diffusion equation:

$$\frac{\partial C(x,y,t)}{\partial t} = D\frac{\partial^2 C(x,y,t)}{\partial x^2} + D\frac{\partial^2 C(x,y,t)}{\partial y^2}, \tag{10}$$

where *x, y* is the position coordinate. The solution to (10) with the point initial concentration b/l^3 (with $l = 1\ \mu\text{m} = 10^{-6}\,\text{m}$) at the point (x,y), is

$$C(x,y,t) = \frac{b/l^3}{4\pi Dt} e^{-d^2/4Dt}, \tag{11}$$

where $d = \sqrt{x^2+y^2}$. The maximum concentration of bacteria when all the grids of the lattice with side length $l = 10^{-6}$ m are filled is $B = l^{-3} = 10^{18}$ m^{-3}. Thus the maximum absorption (infection) rate is $\beta = Bk = 47.5$ s^{-1}, yielding the mean time to absorption $t_a = (\log b)/\beta = 0.0715$ s. The infection radius d^* then satisfies the equation

$$\frac{1}{l^3} = \frac{b}{l^3}\frac{1}{4\pi Dt_a}\exp\left[-\frac{d^{*2}}{4Dt_a}\right], \tag{12}$$

or $d^* = 7.94\ \mu\text{m}$. The infection radius on the lattice is given by the integer part of d^* in units of μm: $d = 7$.

The growth rate of the host, *r*, satisfies the equation:

$$1 + r = 2^{1/t_B}, \tag{13}$$

where t_B is the doubling time of the host. From equation (13), I calculated $r = 0.023$ min^{-1} given that $z_r = 4$, $t_B = 30$ min.